Monolayer instability: An upper bound for the wetting and nonwetting of a substrate by a solid monolayer

James M. Phillips
Department of Physics, University of Missouri–Kansas City, Missouri 64110
(Received 21 July 1994; revised manuscript received 7 November 1994)

Continuum mechanics and computer simulations are used to study the elastic stability of solid monolayers. We observe microscopically the upper limits of the ratio of adsorption to cohesive energies that allow for the wetting of the substrate by a solid monolayer using molecular dynamics. Also, structural instabilities are found analytically in nonlinear elastic continuum models by solving the nonlinear von Kármán equations for a thin circular system (an adsorbed island) undergoing planar compression. The instability occurs as a bifurcation at the first eigenvalue. A series of simulations over a range of adsorbate energies versus temperature demonstrates the existence of a stability boundary.

I. INTRODUCTION

The wetting or nonwetting of substrates by liquid adsorbates has been studied extensively for a very long time, and remains a current topic of interest.[1] However, there have been far fewer investigations of solid films. During computer simulation studies of the microscopic properties of thin solid films, we see the results of structural instability, i.e., monolayers coalescing into other forms.

Our simulations of adsorbates with sufficiently high cohesive energies and at temperatures above their bulk triple point form sessile drops. In the same systems at low temperatures, we find that the solid monolayer is unstable, and observe the system to form terraced islands of multilayer.

We have attempted to understand the physical origins of the crossover from those systems that remain an elastic monolayer to those which become thin terraced multilayers. To this end, we also studied nonlinear elastic continuum models. These models exhibit instabilities in the form of eigenvalue bifurcations. For sufficiently high cohesion in the adsorbate, solid monolayers may actually be near such a bifurcation instability. We believe our qualitative study suggests the existence of a thermomechanical instability as part of the mechanism for the nonwetting of certain solid monolayers. Highly attractive adsorbate molecules are drawn to each other rather than to the less attractive substrate. From a computational point of view, a simulation that starts as a solid monolayer, but cannot remain so, represents a system above the upper bound of scaled interactions possessing monolayer stability. Such monolayers would not wet that particular substrate. In the continuum model, strong adsorbate attraction causes an internal compressive stress. In elastic theory, the body buckles when the compressive stress reaches the first eigenvalue. In our case, the system crumbles. Eigenvalue bifurcation marks the upper bound to the continuum model's stability.

One should note that the static buckling of the continuum model is preempted in the simulations (and in experiment) by thermal fluctuations. We add that feature to the model as a linear perturbation. Physisorbed solids that are far from this unstable region simply respond to modest increases in temperature and compression (spreading pressure) by the transport of molecules into a higher position by the well-studied process of layer promotion.

In Sec. II, we discuss some of the microscopic features of layer promotion in film growth. A short review of interfacial elasticity that helps guide our thinking on this problem is given in Sec. III. We present our results from simulation in Sec. IV A and those from elastic theory in Sec. IV B. Section V contains our discussion of the results.

II. LAYER PROMOTION IN ADSORBATES

When a wetting monolayer is slightly compressed or heated (the system chemical potential is increased), the adsorbate begins a layering transition. This is to say that some of the atoms or molecules in the monolayer are promoted vertically to form a second layer. The atoms from below or others from the coexisting vapor find the upper layer to be energetically favorable. Consequently, they reside there. Such transitions are marked by layering coexistence, and the condition is indicated experimentally by adsorption isotherm steps.

Our simulations show three different microscopic mechanisms for layer promotion occurring under a variety of thermodynamic circumstances (see Fig. 1). First and most often in strongly attractive adsorbates, we

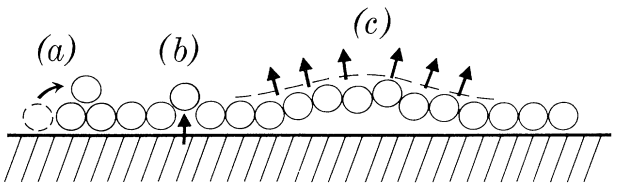

FIG. 1. A diagram illustrating the three microscopic mechanisms for layer promotion observed in our simulations: (a) vertical migration at a free edge, (b) random vertical promotion of individual molecules from increased temperature, and (c) sectional (collective) layer promotion due to elastic instabilities.

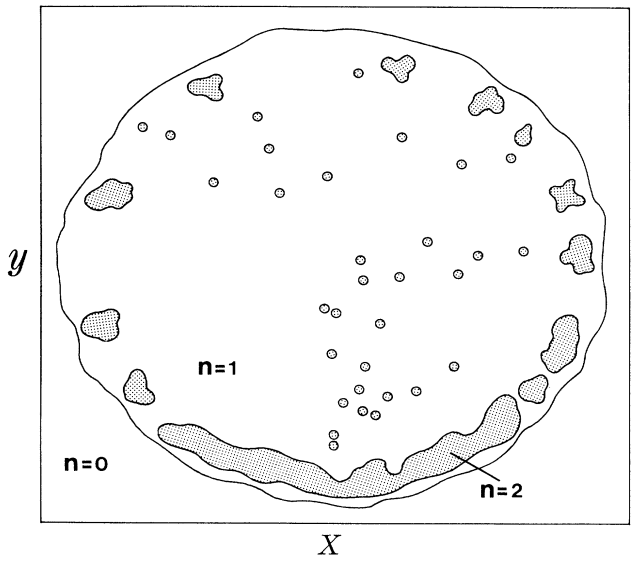

FIG. 2. A final configuration of a solid monolayer showing layer promotion by the (a) and (b) mechanisms in Fig. 1. The system is 5000 atoms at a reduced temperature $t=-0.36$. This is below the bulk triple point of the adsorbate.

observe the atoms on the edges of adsorbed islands to be more likely to migrate to the second layer by simply climbing over their interior neighbors. Second, with sufficient temperature, individual atoms in the interior of the island will randomly gain enough vertical displacement to thermally promote to the upper layer. This appears to be more rare than the edge migration. Figure 2 is the final configuration of a simulation for an argon/graphite monolayer at

$$t=(1-T/T_t)=-0.36$$

reduced temperature. The bulk triple point temperature of the adsorbate is T_t. Both layer promotion mechanisms (a) and (b) of Fig. 1 are present. The simulations use the Nosé molecular dynamics algorithm described in a previous paper.[2] The boundary is a circular system of 5000 particles surrounded by a power-law repulsive potential.[2]

Third, we observe highly compressed solid layers to promote groups of atoms to the second layer in a sudden response to some structural instability. It is this final mechanism that prompted our study. We hope to show that this sudden upheaval is due to an eigenvalue bifurcation in the elastic stability of the film. The details of our analysis of this phenomena are given in Sec. IV.

III. INTERFACIAL ELASTICITY

The role of elasticity in the structure and stability of physically adsorbed layers has rarely been a consideration. However, there is considerable evidence from a variety of surface systems that the stresses and strains in films are important. Early reviews by Herring[3] and Mullins[4] have clarified the thermodynamical and elastic properties of free metal surfaces. One of the many important points they made is the relationship between the surface tension γ and the components of the surface stress σ_{ij}. For a linear elastic isothermal isotropic solid-vapor interface at equilibrium,

$$\sigma_{ij}=\gamma\delta_{ij}+\frac{\partial\gamma}{\partial\varepsilon_{ij}},\quad i,j=1,2\ , \tag{1}$$

where ε_{ij} is the corresponding surface strain. The derivative $\partial\gamma/\partial\varepsilon_{ij}$ is the key to many issues. For example, in liquids $\partial\gamma/\partial\varepsilon_{ij}=0$, indicating the equivalence of surface tension and surface stress. When $\partial\gamma/\partial\varepsilon_{ij}<0$, Andreussi and Gurtin[5] show a flat surface to be unstable and thus predict the conditions for surface wrinkling. Marks, Heine, and Smith[6] later observed the wrinkling of a Au(111) surface under certain conditions. Recent diffraction studies by Mochrie and co-workers[7] show structural changes in strained surface phases on Au(111) and Pt(111). Spencer, Voorhees, and Davis[8] observed morphological instabilities in growing epitaxially strained films. The buckling of Langmuir monolayers[9] and polymerized monomolecular films[10] has been studied successfully with experiments and theory.

Elastic stress induced into adsorbed films by substrate potentials was addressed theoretically by Huse,[11] and in many simulations by Grabow and Gilmer.[12] Gilmer[13] has thoroughly reviewed the role of the misfit and the variation of interactions W on film growth. The ratio $W=\varepsilon_{as}/\varepsilon_{aa}$, where ε_{as} is the potential minimum for the adsorbate-substrate interaction and ε_{aa} is the same for the adsorbate-adsorbate intermolecular potential. Gilmer and co-workers have simulated film growth by molecular-beam deposition, whereas our simulations monitor the results of applying temperature and spreading pressure to an originally static film. They[12] also simulate silicon using the Stillinger-Weber potential.

In our study, we are only dealing with a very thin (1–6 layers) solid films on an essentially rigid but modulated substrate (graphite). However, we believe the work cited above on polymers, metals, and semiconductors suggests an important direction. That is, the structural stability of solid adsorbed film depends strongly on elasticity as well as thermodynamic and kinetic considerations. Wortis[14] has cautioned that care should be exercised in making detailed parallels between the surfaces of bulk systems and island films of finite thickness. We have attempted to use simulation to observe the microscopic behavior of these films, while going to continuum mechanics to qualitatively understand the stability criteria.

IV. STRESS-INDUCED RUPTURE OF ADSORBED FILMS

Recent attention to bifurcation phenomena in physics literature has often centered on sudden changes in the behavior of nonlinear oscillating systems. However, the study of bifurcation theory in nonlinear eigenvalue problems also has a very rich history when applied to the stability limits of physical equilibrium.[15]

When very thin films are subjected to high lateral compression, catastrophic breakup may occur. Such high compressive forces could be achieved through

confining surface geometries, buffer gases applying high spreading pressures, or high cohesive forces in the adsorbate. In our simulations, we use two different approaches. One increases the relative strength of the adsorbate-adsorbate pair interaction relative to the adsorbate-substrate atom-atom potential. The other controls the radius of the circular simulation cell or the box size in a rectangular cell. The contraction of the cell walls increases the pressure within the cell.

A. Molecular-dynamics results

Most of the results presented in this paper start from a monolayer with a high cohesion energy and a relatively weaker interaction with a corrugated graphite substrate. The adsorbate interaction parameter ε—in a Lennard-Jones (LJ) (12,6) potential—is increased, while keeping the holding potential the same. With these interactions fixed, we compute a series of simulations over a range of reduced temperatures t. The reduced temperature increases in increments of 0.10 over a range from -0.8 to $+0.2$. In the Lennard-Jones system the triple point is 0.7ε. The temperature series is then repeated after increasing the adsorbate-adsorbate interaction (ε) by factors from 2 to 10 in increments of 1.0. We computed 77 simulations in this part of the study. The ratio of the adsorbate-adsorbate ε_{aa} to the adsorbate-substrate ε_{as} is scaled from a common reference system, argon adsorbed on graphite. With this factor we increase the strength of the cohesion of the film as a multiple of the base argon/graphite system. For values of the ratio W from one-third to one-tenth in the range of intermediate temperatures below the triple point, we find a region where the third type of layer promotion—part (c) of Fig. 1—is a major factor in the terracing of the film due to elastic instabilities. This system is nonwetting as a solid monolayer.

It was interesting to simulate a nonwetting fluid system to serve as a reference. Starting with an ordered monolayer, the system melts and equilibrates as a sessile droplet. Figure 3 is a picture of the final configuration. This fluid system has ε_{aa} three times that of argon. The temperature is just above the bulk triple point.

Figure 4 is the final configuration of the same system in Fig. 3, except that the temperature is below the bulk triple point of the adsorbate. The simulation began with a solid monolayer and three times the adsorbate attraction of argon. This makes the factor W one-third that of the argon graphite system. The system would not wet the substrate because the internal cohesion of the adsorbate was too great. However, a similar simulation remained a solid monolayer when the W factor is one-half that of the argon/graphite reference system. The interesting feature of the configuration in Fig. 4 is the fact that the center of the circular island has ruptured, and the formation of an annular ring of terraced solid multilayer surrounds a patch of bare substrate. This unusual structure is common in the range of W less than one-third that of argon/graphite. The higher cohesive adsorbates do not remain solid monolayers. As we shall see in Sec. IV B, the maximum amplitude of the buckling displacement

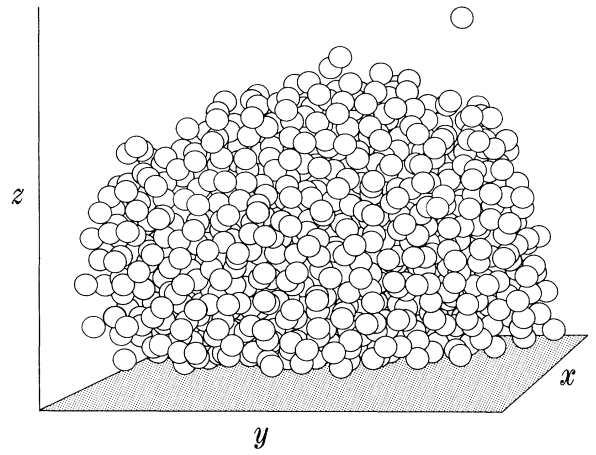

FIG. 3. The final configuration of the sessile drop formed from 5000 atoms at a temperature slightly above the bulk triple point of the adsorbate. The adsorbate interaction is three times that of argon. The interaction to the substrate is the same as argon to graphite. The adsorbate has formed a sessile drop with a visible contact angle.

occurs in the central area of the film. The first region to crumble occurs in the middle of the circle. These molecules are then more mobile, and the film coalesces into the annular multilayer. Other overlapping structures form. The film has, on occasion, ruptured along a diameter through the circular island and left a solid band of terraces across the film. After many simulations, our heuristic conclusion is that the film can only take up to a

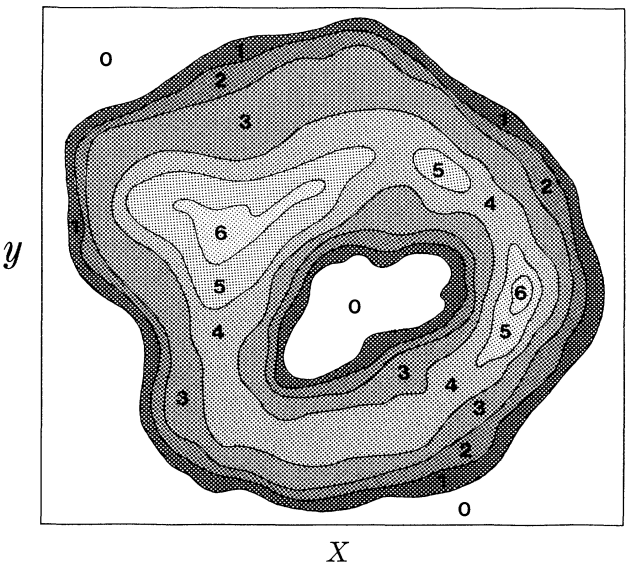

FIG. 4. A final configuration for the system in Fig. 3 but at a temperature below the bulk triple point of the adsorbate. The reduced temperature is $t=-0.36$. The numbers indicate the layers existing above the substrate ($n=0$). These contours were drawn from atom positions of the resulting terraced solid multilayer.

critical value of in-plane pressure. Once exceeded, the film crumbles into a more tolerant multilayer or to a bulk solid if there are sufficient atoms present. This pressure is internally generated in these simulations, but we also report that by tightening the in-plane boundaries on circular or rectangular simulation cells we have increased the pressure externally. Similar results are obtained. In order to examine the existence of such a critical compression limit, we turn to continuum mechanics.

B. Analytic studies of the continuum model

We model the film as a circular elastic continuum of radius R and thickness h. Until the monolayer begins to break up due to the applied in-plane stress and/or increased temperature, the continuum model is quite instructive. The material is assumed to be isotropic and has a Poisson's ratio (ν). The perimeter of the film is subject to an in-plane radial stress. This applied stress substitutes for the compression of the monolayer by its own cohesive pair interactions and a spreading pressure. Assuming a density of atoms ρ with the attractive part of the pair interaction given by

$$\phi \approx -4\varepsilon \left[\frac{\sigma}{r} \right]^6 ,$$

the radial stress applied to a central core of radius r_0 is approximated by

$$S(r_0) \approx -\frac{4\varepsilon\rho h}{2} \int_{r_0}^{\infty} \nabla\phi 2\pi r \, dr = \varepsilon\alpha ,$$

where α is a constant. Hence, if we take systems with an increased pair parameter ε, we increase the radial stress proportionally.

The plate is mechanically stable unless the radial stress reaches a critical value. At that level, the plate buckles. In the molecular system, if the ε_{aa} is too great, the monolayer is not a mechanically stable structure. This mechanical condition implies the thermodynamic condition that the adsorbate no longer wets the substrate. The critical stress or critical ε_c not only must exceed the elastic limit but must also exceed the additional stabilizing influence of the holding potential of the substrate. When the system is driven to the buckling condition, that ends the comparison of the continuum model to the adsorbate system. The molecular monolayer will not resist fragmentation, as would a metallic plate. The point is that the buckling conditions are an upper limit to the thermomechanical condition for the monolayer to wet the substrate. In fact, one would expect thermal fluctuations to preempt this static limit. Solutions to the continuum model require the nonlinear elastic equations given by von Kármán.[16] We follow the solution given by Stoker.[15] In Cartesian coordinates, assuming the middle of the plate is $z=0$, then the von Kármán equations are written

$$\nabla^4\phi = \frac{\partial^2 w}{\partial y^2}\frac{\partial^2 w}{\partial x^2} - \left[\frac{\partial^2 w}{\partial x \partial y} \right]^2$$

and

$$(\Gamma h)^2 \nabla^2 w - \frac{\partial^2\phi}{\partial y^2}\frac{\partial^2 w}{\partial x^2} + 2\frac{\partial^2\phi}{\partial x \partial y}\frac{\partial^2 w}{\partial x \partial y} - \frac{\partial^2\phi}{\partial x^2}\frac{\partial^2 w}{\partial y^2} = 0 .$$

The components of the displacement of an infinitesimal volume of the middle surface of the plate are (u,v,w). The function ϕ is the elastic stress function. The following derivatives are the components of the accompanying stresses divided by Young's modulus:

$$\sigma_{xx} = \left[\frac{\partial^2\phi}{\partial y^2} \right], \quad \sigma_{xy} = -\left[\frac{\partial^2\phi}{\partial x \partial y} \right], \quad \sigma_{yy} = \left[\frac{\partial^2\phi}{\partial x^2} \right]$$

and

$$\Gamma^2 = [12(1-\nu^2)]^{-1} .$$

The relations between the strains, displacements, and stresses are

$$\varepsilon_{xx} = \left[\frac{\partial u}{\partial x} \right] + \frac{1}{2}\left[\frac{\partial w}{\partial x} \right]^2 = -\sigma_{xx} + \nu\sigma_{xy} ,$$

$$\varepsilon_{xy} = \frac{1}{2}\left[\frac{\partial u}{\partial y} + \frac{\partial v}{\partial x} + \frac{\partial w}{\partial x}\frac{\partial w}{\partial y} \right] = -(1+\nu)\sigma_{xy} ,$$

and

$$\varepsilon_{yy} = \left[\frac{\partial v}{\partial y} \right] + \frac{1}{2}\left[\frac{\partial w}{\partial y} \right]^2 = -\sigma_{yy} + \nu\sigma_{xx} .$$

Converting to polar coordinates,

$$\begin{aligned} &\mathfrak{L}p = \tfrac{1}{2}q^2 , \\ &\eta^2 \mathfrak{L}q + pq = 0 , \end{aligned} \tag{2}$$

where

$$p = \frac{1}{r}\left[\frac{\partial\phi}{\partial r} \right], \quad q = \frac{R}{r}\left[\frac{\partial w}{\partial r} \right], \quad \eta = \frac{\Gamma h}{R}$$

and

$$\mathfrak{L} \equiv R^2 \left[\frac{d^2}{dr^2} \right] + \frac{3}{r}\frac{d}{dr} .$$

Coupled nonlinear equations must be solved simultaneously. Equations [Eq. (2)] with the appropriate boundary conditions formulate the problem. The conditions at the center ($r=0$) are

$$\left. \frac{dp}{dr} \right|_{r=0} = 0 \quad \text{and} \quad \left. \frac{dq}{dr} \right|_{r=0} = 0 \tag{3a}$$

since the system has radial symmetry. The functions ϕ and w have continuous fourth derivatives. At the plate edge, $r=R$,

$$p = \bar{p} \quad \text{and} \quad \left. r\frac{dq}{dr} + (1+\nu)q \right|_{r=R} = 0 , \tag{3b}$$

where the last equation states the vanishing of the bending moment at the plate edge. Solving for p and q will determine all physics of the problem. The stress at the circumference is

$$p_c = r\left[\frac{dp}{dr}\right] + p \ .$$

The radial bending stress and the bottom of the plate is

$$p_b = 6\gamma\eta\left[r\frac{dp}{dr} + (1+\nu)q\right] ,$$

and the normal deflection (buckling) is

$$w = \frac{1}{R}\int_r^R qr\,dr \ .$$

The important parameters are Poisson's ratio ν and the eigenvalue

$$\lambda^2 = \bar{p}/\eta^2 ,$$

which is our driving criteria—the in-plane compression.

The boundary value problem is properly posed. For sufficiently small values of λ^2, the in-plane compression is the only solution—$w=0$. As λ^2 increases, nontrivial solutions arise in which $w\neq 0$. The plate buckles with a finite distribution of vertical displacement. In our application, only the first eigenvalue is germane. Thus perturbation theory is best suited for our analysis.

Usually, there are two symmetric solutions $\pm q$. In our case, the substrate constrains out the negative slope of the vertical deflection. Assume that the functions p and q to be expanded as a series in a small parameter ε, and require that $\varepsilon\to 0$ at the onset of buckling. We write

$$\begin{aligned} q &= \varepsilon q_1 + \varepsilon^3 q_3 + \varepsilon^5 q_5 + \cdots , \\ p &= p_0 + \varepsilon^2 p_2 + \varepsilon^4 p_4 + \cdots , \\ \bar{p} &= \bar{p}_0 + \varepsilon^2 \bar{p}_2 + \varepsilon^4 \bar{p}_4 + \cdots . \end{aligned} \tag{4}$$

In this formalism, $\bar{p}=\bar{p}_0$ is the value of the edge force that starts the buckling.

Substitute Eq. (4) into Eq. (2) and the boundary conditions Eq. (3a) and (3b) and separate out the orders in powers of ε. The zeroth-order equation is

$$\mathfrak{L} p_0 = 0 ,$$

and the companion zeroth-order boundary conditions are

$$\left.\frac{dp_0}{dr}\right|_{r=0} = 0 \quad \text{and} \quad p_0 = \bar{p}_0 .$$

The general solution is

$$p_0 = \frac{C_1}{r^2} + C_2 .$$

The singularity at the origin is incompatible with the first boundary condition, and in the second boundary condition gives $C_2=\bar{p}_0$. The zeroth-order solution is as yet an unknown constant. This solution has no vertical deflection and is equivalent to the linear elastic problem. The eigenvalue and, consequently, the in-plane compression are still too small to initiate vertical displacement.

For increased compression, we rewrite the first-order equation to be

$$\rho^2\frac{d^2\theta}{d\rho^2} + \rho\frac{d\theta}{d\rho} + (\rho^2-1)\theta = 0 , \tag{5}$$

which is the first-order Bessel's equation. Here

$$\rho \equiv \lambda_0 r/R, \quad \theta \equiv q_1 r/R, \quad \text{and} \quad \lambda_0^2 = p_0/\eta^2 .$$

The first-order boundary condition at the plate edge is

$$\lambda_0 J_0(\lambda_0) - (1-\nu)J_1(\lambda_0) = 0 . \tag{6}$$

The roots of this transcendental equation are the bifurcation eigenvalues of our boundary value problem. For example, for values of Poisson's ratio, assume $\nu=0.2$ and 0.3. The critical compression is $\bar{p}_0 = 0.0297(h/R)^2$ and $0.0352(h/R)^2$, respectively. This value would be the upper limit of the perimeter radial stress or, proportionally, the upper limit of $W=\varepsilon_{aa}/\varepsilon_{as}$ which allows the monolayer to wet the substrate. Finite-sized islands of adsorbate that are stabilized by the holding potential will have a threshold of in-plane compression.

A description to the linear compression up to the critical buckling value is realized by first-order theory. Until the compression reaches the first eigenvalue, the solution is the trivial $q_1=0$. The plate is flat to the substrate. At the first eigenvalue, the amplitude of first-order solution is finite, and to this level of approximation is

$$q_1 = \frac{C_1 R}{r} J_1(\lambda_0 r/R) . \tag{7}$$

We have carried out the solution to the eight order and have shown the correction to be less than 10%. The profile is not important to our microscopic film of atoms because the monolayer crumbles. This is demonstrated in the simulations. Linear (first-order) theory predicts the existence and magnitude of the eigenvalue bifurcation, but it takes nonlinear higher-order theory to solve for the plate profile.

The second-order equation

$$\mathfrak{L} p_2 = \tfrac{1}{2} q_1^2 , \tag{8}$$

with

$$\frac{dp_2}{dr} = 0 ,$$

also has a closed-form solution

$$\begin{aligned} p_2 = {} & \tfrac{1}{8}[1 + J_0^2(\lambda_0 r/R)] - \tfrac{1}{4}[J_0(\lambda_0 r/R) + J_1(\lambda_0 r/R)] \\ & + \tfrac{1}{8}[J_0(\lambda_0 r/R) J_2(\lambda_0 r/R)] + C_1 + \frac{C_2}{(\lambda_0 r/R)^2} . \end{aligned} \tag{9}$$

The constant $C_2=0$. For higher-order solutions, we have used power series.

To observe the bifurcation at the first eigenvalue graphically, the first equation in Eq. (4) is inverted for ε as a series in q_i. This approximation for ε is substituted into the second equation of Eq. (4) to obtain the radial stress as a function of the slope of the vertical displacement. Evaluation at the plate edge gives the applied stress as a function of vertical displacement (buckling). To the lowest order of approximation, this relationship is

quadratic and is given by

$$\bar{p} \approx \bar{p}_0 + \left[\frac{q}{q_1}\right]^2 + \cdots . \tag{10}$$

Figure 5 shows the bifurcation at the critical stress $\bar{p}_0$, i.e., the first eigenvalue. Recall that the negative vertical displacements are constrained because of the substrate. In our system, the higher-order bucklings are academic since our monolayer no longer exists as a structure after the compression reaches the first eigenvalue.

Eigenvalue bifurcations as critical values in structural problems date to Euler and Bernoulli. Experimental systems under compressive stresses respond elastically with linear displacements until the critical value is exceeded. Once surpassed, the system displacements become large-amplitude departures from the linear case. For different geometries, the location of eigenvalues can be simple or highly detailed. In one dimension, (buckling columns) the first eigenvalue is

$$\lambda_n = (n\pi)^2, \quad n = 1,2, \ldots .$$

For a two-dimensional rectangular plate[17] (h) thick, length (a) and width (b), the eigenvalues are

$$\lambda_{mn} = \left[\frac{E}{12(1-\nu^2)}\right]\left[\frac{\pi h}{a}\right]^2\left[m + \frac{n^2a^2}{mb^2}\right]^2 .$$

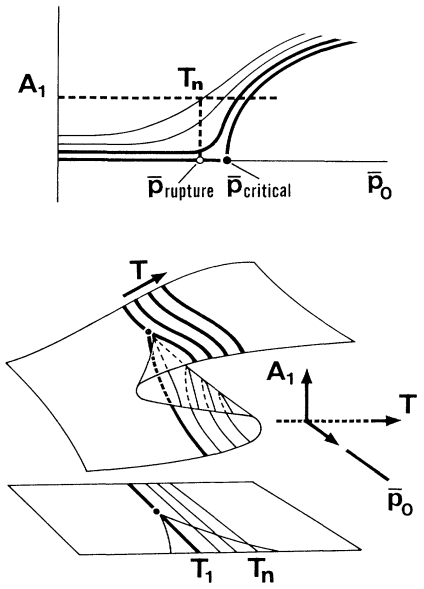

FIG. 5. The three-dimensional figure is a schematic diagram of the potential-energy sheet $V(A_1, \bar{p}_0, T)$ in terms of the amplitude of the buckling A_1, the radial stress $\bar{p}_0$, and the temperature $T \propto \delta$. The diagram shows the bifurcation of the film's vertical displacement $w \propto A_1$ as a function of stress $\bar{p}_0$ applied to the rim. The two-dimensional projection of A_1 vs $\bar{p}_0$ is the usual bifurcation pitchfork. The lower prong of the pitchfork is not allowed because of the presence of the substrate. The additional lines are profiles with thermal fluctuations included. The theoretical bifurcation point $\bar{p}_{\text{critical}}$ and the physical rupture point $\bar{p}_{\text{rupture}}$ are shown.

The first (critical) eigenvalue is for $n = m = 1$. E is Young's modulus, and ν is again Poisson's ratio. We have previously published a picture from the simulation of a rectangular film that was initially compressed beyond its stability point (see Fig. 4 of Phillips and Hruska).[18]

Continuum models are by their nature idealizations of a molecular system. In order to move the model closer to the simulation and to experiment, we attempt to include the effects of thermal fluctuations into the continuum bifurcation model. The effects of temperature (in particular, the vertical amplitudes of the mean-square displacement of the atoms) on molecular monolayers introduce another variable into the bifurcation phenomenon. The concept is just that used in structural mechanics to include material imperfections. A monolayer is not perfectly flat, vertical displacements of the atoms prevent the system from being in a mathematically flat plane. Thus, the zero norm for the solutions, until the critical compression has been reached, is not precisely true in our application. The vertical component of the mean-square displacements of atoms in a solid monolayer due to thermal vibrations (phonons) is an additional disordering feature present in our simulations and in experiment. We include these effects in our continuum model as a first-order perturbation to the energy of the strained system.

For clarity and simplicity, consider the one-dimensional case mentioned above. The potential energy for the one-dimensional example is a function of the derivatives of the longitudinal displacement u and the vertical displacement w:

$$V = \tfrac{1}{2}\int_0^l [(w_{xx})^2 + (u_x + w_x^2/2)^2]dx ,$$

where l is the length of the rod. The work required to so contort the one-dimensional strip is given in terms of the difference between the original length l and the shortened curvilinear length L:

$$\Delta W = \int_L^l \bar{p}_0 dx = \bar{p}_0(L - l) .$$

This resulting length is

$$L = \int_0^l \sqrt{1 + w_x^2}dx = \int_0^l [1 + w_x^2/2 - w_x^4/4 + \cdots]dx .$$

Then

$$L = l + \tfrac{1}{2}\sum_{n=1}^{\infty} A_1^2 (n\pi/l)^2 (l/2) + \cdots ,$$

where the nth eigenfunction is

$$w_n(x) = A_n \sin(n\pi x/l) .$$

Written as an expansion in the amplitude of the first eigenfunction, the potential energy is

$$V(A_1, \bar{p}_0) \approx (l/4)(\pi/l)^2(\bar{p} - \bar{p}_0)A_1^2 + (3\bar{p}_0 l/2^6)(\pi/l)^4 A_1^4 + \cdots .$$

Now, if the effects of microscopic perturbations in the energy δ are added, at least to the linear term, one obtains

$$V(A_1, \bar{p}_0, \delta) \approx A_1\delta + \cdots + (l/4)(\pi/l)^2(\bar{p} - \bar{p}_0)A_1^2 + (3\bar{p}_0 l/2^6)(\pi/l)^4 A_1^4 + \cdots .$$

On the microscopic scale, we identify the perturbing imperfections as thermal fluctuations $\delta \propto T$. The higher the temperature, the greater the amplitude of the vertical displacement becomes. When this amplitude exceeds some critical displacement, the solid film crumbles in a rather catastrophic manner. This is represented by a dashed line on the amplitude A_1 in Fig. 5. The limit is not unlike a Lindemann criterion. The point is merely that with an experimental system, thermal fluctuations preempt the strict mathematical limit of $\bar{p}_{\text{critical}}$. The amplitude solution curve is raised, and its intersection with the assumed limit predicts a realistic limit $\bar{p}_{\text{rupture}}$.

If the three-variable function of the potential energy is plotted, we observe that Eq. (10) is a two-dimensional projection for the function sheet of $V(A_1,\bar{p}_0,\delta)$ (see Fig. 5). We have used the temperature in place of δ. In the amplitude versus compression projection of our energy function (Fig. 5), the dotted line represents the critical amplitude for stability. The curve of the cross-sectional region represents the imperfect film's departure from the pitchfork of the pure mathematical solution. The higher contours represent higher temperatures. The upper limit of the transition from a wetting solid monolayer to a nonwetting one is achieved when the cohesive energy and/or temperature combination drives the vertical displacement amplitude of the film to the critical bifurcation limits shown in Fig. 5. At $T=0$, the limiting compression $\bar{p}_{\text{critical}}$ is the critical eigenvalue. At the higher temperatures, the contours are intercepted at a stress value $\bar{p}_{\text{rupture}} < \bar{p}_{\text{critical}}$.

V. DISCUSSION

The logic of our simple qualitative modeling is elementary. If the starting configuration of the system is a monolayer at a given set of conditions (temperature, interaction strengths, etc.), will the film essentially remain a monolayer? If so, these conditions are representative of possible wetting by a solid phase. If not, then the given system is beyond the upper limit of wetting. We qualify our conclusion for a wetting system to be only an upper limit because it is quite possible that a system that starts as a monolayer might not be experimentally achievable in an atom by atom adsorption. Hence we reserve the observed conditions in our simulations merely as an upper limit since we use the solid monolayer as a starting configuration.

It would be helpful to have a simple and readily available scaling for the wettability of solid physisorbed monolayers. Interaction potentials for many systems are not well known, and the quantitative determination of them is often laborious. What one needs is a relatively common pair of thermodynamic results that give a relative measure of the molecules' energy with the substrate versus their energy with each other. Although many such values exist, we have arbitrarily chosen the isosteric heat in the low coverage limit, and the latent heat of fusion at the triple point.

Table I lists these ratios for several commonly adsorbed systems on graphite or carbon black. Nitrogen and methane each have a ratio slightly more than three

TABLE I. Experimental values and the wettability ratio for example systems on graphite or carbon black.

Adsorbate	Isosteric heat in the low coverage limit (cal./mole)	Latent heat at the triple point (cal./mole)	Ratio
Methane	2900	225.5	12.86
Nitrogen	2200	171.6	12.82
Argon	2300	280.8	8.19
Krypton	3100	390.7	7.93
Xenon	4000	548.5	7.29
Ethane	4230	683	6.19
Ethylene	4000	800.8	5.00
Water	4000	1435.7	2.79
Ammonia	3960	1424	2.78
Carbon dioxide	4000	1928	2.07

halves of the rare gases. The particular point of interest is that the factor for ammonia is one-third that of the argon system, and just over one-fifth that of nitrogen and methane. In our simulation, the factor $W=\varepsilon_{as}/\varepsilon_{aa}$ was used. We found the instability when ε_{aa} of the argon graphite system was multiplied by three, but that the solid monolayer wetted the graphite when only multiplied by two. The adsorbate-substrate parameter was kept the same in all simulations. With these dissimilar ratios as guides, the nitrogen and methane systems would be expected to wet graphite even more readily than do the rare gases. As an example of the nonwetting of a monolayer at low temperatures, our model suggests stronger adsorbate interactions or weaker interaction with the substrate. Ammonia on graphite is in the region of questionable wettability according to our simulations. It is quite interesting that recent neutron-diffraction experiments by Larese, Hastings, and Phillips[19] do not find a signal consistent with the formation of a two-dimensional solid phase. To this time, the existence of a solid ammonia monolayer adsorbed on graphite remains a controversial problem in spite of a sizable body of work.[20]

The experimental evidence for the wetting of the substrates by solid monolayers has been discussed in broader reviews by Larese,[21] Hess,[22] Thomy and Duval,[23] and Sinha.[24] The present status of the noble-gas adsorbates is that their solid monolayers definitely wet graphite. In fact, there is ample evidence that films of several solid layers grow through a succession of isothermal steps.[21–24]

Our model predicts that the low-temperature (solid) monolayers of heavier noble gases should all wet graphite. Their ratios in Table I are nearly equal. The argon/graphite system was studied by early monolayer isotherms[25] and more recently by Zhang and Larese[26] and Youn, Meng, and Hess.[27] X-ray,[28] neutron,[29] and low-energy electron-diffraction[30] (LEED) experiments demonstrate the existence of the solid monolayer. The structural case for solid monolayers of Kr/graphite is made by LEED,[31] high-energy electron diffraction (HEED),[32] x-ray diffraction,[33] and isothermal steps by Larher,[34] Thomy and Duval,[35] and Hess.[27] Xenon monolayers are also

known to wet graphite from the sharp steps in low-temperature isotherms. Diffraction experiments[36] and thermodynamic studies[37] likewise confirm the existence of the two-dimensional solid.

Methane and nitrogen adsorbates have nearly equal ratios in Table I. The value is over 50% higher than for the noble gases. Our model suggests that a monolayer of methane or nitrogen should wet more readily than even the noble gases. Neutron diffraction by Kjems *et al.*[38] demonstrated the presence of a solid monolayer of nitrogen on graphite. In addition, LEED (Ref. 39) and reflection high-energy electron-diffraction (RHEED) (Ref. 32) experiments confirm the existence of the expected solid nitrogen monolayer. Steele[40] quotes the effective difference in the intermolecular pressure from the first to second layers of nitrogen to be 60 atm. This high level of internal stress in very thin films which shows up in the data from N_2 (Ref. 41) and CH_4 (Ref. 42) experiments. Once the film grows to a sufficient thickness where the top of the film does not feel the substrate potential as strongly, the differences in the shearing stresses between layers of the film are so great that the upper layers may become incommensurate with the lower layers.[43] This seems to be the case for CH_4.[42] In nitrogen, the loss of compression at the top of the film appears to induce partial wetting by growing β bulk.[41]

Vora, Sinha, and Crawford[44] observed solid methane monolayers by neutron diffraction.[45] Larese *et al.*[42] recently completed a series of experiments for coverages extending to trilayers. Gay *et al.*[46] used electron-diffraction methods to study methane films and found diffraction patterns consistent with solid monolayers. In these films (see Table I), experiments show clearly the readiness of adsorbates with their ratios in the 8–12 range to form solid monolayers at temperatures well below the bulk triple point.

Ethane and ethylene at low temperatures have regions of low (horizontal) and high (vertical) density solid monolayer phases. In Table I, they have ratios in the five 5–6 range that suggests a consistency with our continuum model prediction. These ratios are only 25% and 40% less than those of the noble-gas systems. Larese and coworkers[47] have taken neutron-diffraction patterns from ethylene films showing ordered $2d$ phases. Low-energy electron-diffraction[48] and computer simulations[49] agree with this interpretation. The total wetting to bulk films appears not to occur below 74 K. Solid ethane films are observed by a number of investigators using neutron diffraction[50] and LEED.[51] Consistent interpretations of heat-capacity[52] and vapor-pressure isotherm[53] experiments for ethane agree with the actuality of the ordered $2d$ solid.

Small polar molecules have an additional absorbate energy in an ordered array due to their mutual electrostatic interactions. At higher temperatures, this contribution to cohesion of the adsorbate is reduced either through layer promotion or rotational disordering. This could account for the reported wetting of graphite by a fluid monolayer at an elevated temperature. This possible effect was pointed out to me by Larese.[19] An example of this static energy was calculated for CO_2 by Bruch.[54] The ratios in Table I for water, ammonia, and carbon dioxide are all at or below one-third the value for argon on graphite. Their adsorbate pair interactions are too strong for the monolayer solid to form. Our model suggests these adsorbates might not wet graphite as a low-temperature solid monolayer. This appears to be the experimental situation. Terlain and Larher[55] find the CO_2 monolayer does not wet graphite below 104 K. Kiselev *et al.*[56] and Avgul *et al.*[57] find that water does not appear to wet graphite. According to our proposed criterion, the last three adsorbates listed in Table I should not form low-temperature solid monolayers on graphite. By comparison, the case for nonwetting by the solid ammonia monolayer may be understood. Other systems with similar ratios do not wet at low temperatures. The ammonia results[19] are consistent with this classification. The first seven adsorbates in Table I should have solid monolayer phases. The experimental evidence is that they do. Our continuum model finds a nonlinear elastic eigenvalue bifurcation as a compressional limit to the formation of a stable film. The simulations demonstrate the crude limits on the interactions for systems where one could reasonably expect to find stable monolayers.

ACKNOWLEDGMENTS

I would like to thank J. Z. Larese for his hospitality and the sharing of his data previous to publication, J. G. Dash for helpful discussions and for providing me with some of his unpublished work on continuum models, and L. W. Bruch for helpful criticism early in this study.

[1]A. W. Adamson, *Physical Chemistry of Surfaces,* 5th ed. (Wiley, New York, 1990); J. S. Rowlinson and B. Widom, *Molecular Theory of Capillarity* (Clarendon, Oxford, 1982); J. Hautman and M. L. Klein, Phys. Rev. Lett. **67**, 1763 (1991).

[2]James M. Phillips and N. Shrimpton, Phys. Rev. B **45**, 3730 (1992).

[3]C. Herring, in *The Physics of Powder Metallurgy,* edited by W. E. Kingston (McGraw-Hill, New York, 1951).

[4]W. W. Mullins, *Metal Surfaces: Structure, Energetics, and Kinetics* (American Society for Metals, Metals Park, OH, 1963).

[5]F. Andreussi and M. E. Gurtin, J. Appl. Phys. **48**, 3798 (1977).

[6]L. D. Marks, V. Heine, and D. J. Smith, Phys. Rev. Lett. **52**, 656 (1984).

[7]K. G. Huang, Doon Gibbs, D. M. Zehner, A. R. Sandy, and S. G. J. Mochrie, Phys. Rev. Lett. **65**, 3313 (1990); A. R. Sandy, S. G. J. Mochrie, D. M. Zehner, K. G. Huang, and Doon Gibbs, Phys. Rev. B **43**, 4667 (1991).

[8]J. Spencer, P. W. Voorhees, and S. H. Davis, Phys. Rev. Lett. **67**, 3696 (1991).

[9]S. T. Milner, J.-F. Joanny, and P. Pincus, Europhys. Lett. **9**, 495 (1989).
[10]L. Bourdieu, J. Daillant, D. Chatenay, S. Braslau, and D. Colson, Phys. Rev. Lett. **72**, 1502 (1994).
[11]D. A. Huse, Phys. Rev. B **29**, 6985 (1984).
[12]M. H. Grabow and G. H. Gilmer, Surf. Sci. **194**, 333 (1988); G. H. Gilmer, M. H. Grabow, and A. F. Bakker, Mater. Sci. Eng. B **6**, 101 (1990).
[13]C. Roland and G. H. Gilmer, Phys. Rev. B **47**, 16 286 (1993).
[14]M. Wortis, in *Phase Transitions in Surface Films 2,* edited by H. Taub *et al.*, Vol. 267 of *NATO Advanced Study Institutes Series B: Physics* (Plenum, New York, 1991).
[15]*Bifurcation Theory and Nonlinear Eigenvalue Problems,* edited by J. B. Keller and S. Antman (Benjamin, New York, 1969); J. J. Stoker, *Nonlinear Elasticity* (Gordon and Breach, New York, 1969); R. W. Dickey, *Bifurcation Problem in Nonlinear Elasticity* (Pitman, San Francisco, 1976).
[16]Th. von Kármán, *Festigkeitprobleme im Maschinenbau* (Teubner, Leipzig, 1910).
[17]L. Bauer and E. L. Reiss, J. Soc. Ind. Appl. Math. **13**, 604 (1965); K. O. Friedrichs and J. J. Stoker, Am. J. Math. **63**, 839 (1941).
[18]James M. Phillips and C. D. Hruska, Phys. Rev. B **39**, 5425 (1989).
[19]J. Z. Larese, J. M. Hastings, and James M. Phillips, Bull. Am. Phys. Soc. **38**, 279 (1993).
[20]G. Bomchil, N. Harris, M. Leslie, J. Tabony, J. W. White, P. H. Gamlen, R. K. Thomas, and T. D. Trewern, J. Chem. Soc. Faraday Trans. 1 **75**, 1535 (1979); J. Tabony, G. Bomchil, N. Harris, M. Leslie, J. W. White, P. H. Gamlen, R. K. Thomas, and T. D. Trewern, *ibid.* **75**, 1570 (1979); P. H. Gamlen, R. K. Thomas, T. D. Trewern, G. Bomchil, N. Harris, M. Leslie, J. Tabony, and J. W. White, *ibid.* **75**, 1543 (1979); P. H. Gamlen, R. K. Thomas, T. D. Trewern, G. Bomchil, N. Harris, M. Leslie, J. Tabony, and J. W. White, *ibid.* **75**, 1553 (1979); P. Rowntree, G. Scoles, and J. Xu, J. Chem. Phys. **92**, 3853 (1990); A. Cheng and W. A. Steele, *ibid.* **92**, 3858 (1990); **92**, 3867 (1990).
[21]J. Z. Larese, Acc. Chem. Res. **26**, 353 (1993).
[22]G. Hess, in *Phase Transitions in Surface Films 2,* edited by T. Taub *et al.* (Plenum, New York, 1991), p. 247.
[23]A. Thomy and X. Duval, Surf. Sci. **299/300**, 415 (1994).
[24]*Ordering in Two Dimensions,* edited by S. K. Sinha (Elsevier, New York, 1980).
[25]Y. Larher, Surf. Sci. **134**, 469 (1983).
[26]Q. M. Zhang and J. Z. Larese, Phys. Rev. B **43**, 938 (1991).
[27]H. S. Youn, X. F. Meng, and G. B. Hess, Phys. Rev. B **48**, 14 556 (1993).
[28]J. P. McTague, J. Als-Nielsen, J. Bohr, and M. Nielsen, Phys. Rev. B **25**, 7765 (1982); M. Nielsen *et al.*, *ibid.* **35**, 1419 (1987); K. L. D'Amico, J. Bohr, D. E. Moncton, and D. Gibbs, *ibid.* **41**, 4368 (1990).
[29]J. Z. Larese and Q. M. Zhang, Phys. Rev. Lett. **64**, 922 (1990); H. Taub *et al.*, Phys. Rev. B **16**, 4511 (1977); C. Tiby and H. J. Lauter, Surf. Sci. **117**, 277 (1982).
[30]C. G. Shaw, S. C. Fain, Jr., and M. D. Chinn, Phys. Rev. Lett. **41**, 955 (1978); C. G. Shaw and S. C. Fain, Jr., Surf. Sci. **83**, 1 (1976); **91**, L1 (1980).
[31]S. C. Fain, Jr., M. D. Chinn, and R. D. Diehl, Phys. Rev. B **21**, 4170 (1980).
[32]J. A. Venables *et al.*, Surf. Sci. **145**, 345 (1984).
[33]P. W. Stevens, P. Heiney, R. J. Birgeneau, and P. M. Horn, Phys. Rev. Lett. **43**, 47 (1979); R. F. Hainsey, R. Gangwar, J. D. Shindler, and R. M. Suter, Phys. Rev. B **44**, 3365 (1991); P. W. Stevens, P. Heiney, R. J. Birgeneau, P. M. Horn, D. E. Moncton, and G. S. Brown, *ibid.* **29**, 3512 (1984).
[34]Y. Larher, J. Chem. Soc. Faraday Trans. I **70**, 320 (1974).
[35]A. Thomy, X. Duval, and J. Regnier, Surf. Sci. Rep. **1**, 1 (1981).
[36]H. Hong, R. J. Birgeneau, and M. Sutton, Phys. Rev. B **33**, 3344 (1986); S. E. Nagler, P. M. Horn, T. F. Rosenbaum, R. J. Birgeneau, M. Sutton, S. G. J. Mochrie, D. E. Moncton, and Roy Clarke, *ibid.* **32**, 7373 (1985).
[37]R. Gangwar, N. J. Colella, and R. M. Suter, Phys. Rev. B **39**, 2459 (1989).
[38]J. K. Krems, L. Passell, H. Taub, J. G. Dash, and A. D. Novaco, Phys. Rev. B **13**, 1446 (1976).
[39]R. D. Diehl and S. C. Fain, Jr., Surf. Sci. **125**, 116 (1983).
[40]W. A. Steele, *The Interaction of Gases with Solid Surfaces* (Pergamon, Oxford, 1974).
[41]U. G. Volkmann and K. Knorr, Phys. Rev. Lett. **66**, 473 (1991).
[42]J. Z. Larese, M. Harada, L. Passell, J. Krim, and S. Satija, Phys. Rev. B **37**, 4735 (1988).
[43]James M. Phillips and N. Shrimpton, Phys. Rev. B **45**, 3730 (1992).
[44]P. Vora, S. K. Sinha, and R. K. Crawford, Phys. Rev. Lett. **43**, 704 (1979).
[45]G. Bromchil, A. Huller, T. Rayment, S. J. Roser, M. V. Smalley, R. K. Thomas, and J. W. White, Philos. Trans. R Soc. London Ser. B **290**, 537 (1980).
[46]J. M. Gay, A. Dutheil, J. Krim, and J. Suzanne, Surf. Sci. **177**, 25 (1986).
[47]J. Z. Larese, L. Passell, A. D. Heidemann, D. Richter, and J. P. Wicksted, Phys. Rev. Lett. **61**, 432 (1988); B. H. Grier, L. Passell, J. Eckert, H. Patterson, D. Richter, and R. J. Rollefson, *ibid.* **53**, 814 (1984); S. K. Satija, L. Passell, J. Eckert, W. Ellenson, and H. Patterson, *ibid.* **51**, 411 (1983); J. Z. Larese, L. Passell, and B. Ravel, Can. J. Chem. **66**, 633 (1988).
[48]V. L. Eden and S. C. Fain, Jr., Phys. Rev. B **43**, 10 697 (1991).
[49]M. A. Moller and M. L. Klein, Chem. Phys. **129**, 235 (1989); A. Cheng and M. L. Klein, Langmuir **8**, 2798 (1992); S. Nosé and M. L. Klein, Phys. Rev. Lett. **53**, 818 (1984).
[50]J. P. Coulomb, J. P. Biberian, J. Suzanne, A. Thomy, G. J. Trott, H. Taub, H. R. Danner, and F. Y. Hansen, Phys. Rev. Lett. **43**, 1878 (1979); H. Taub, G. J. Trott, F. Y. Hansen, H. R. Danner, J. P. Coulomb, J. P. Biberian, J. Suzanne, and A. Thomy, in *Ordering in Two Dimensions,* edited by S. K. Sinha (Elsevier, New York, 1980); G. J. Trott, Ph.D. thesis, University of Missouri-Columbia, 1981; J. Suzanne, J. L. Seguin, H. Taub, and J. P. Biberian, Surf. Sci. **125**, 153 (1983); J. M. Gay, J. Suzanne, and R. Wang, J. Phys. (Paris) Lett. **46**, L425 (1985); J. M. Gay, J. Suzanne, and R. Wang, J. Chem. Soc. Faraday Trans. 2, **82**, 1669 (1986).
[51]J. W. Olsen and S. C. Fain, Jr., Phys. Rev. B **36**, 4074 (1987).
[52]S. Zhang and A. D. Migone, Phys. Rev. B **38**, 12 039 (1988).
[53]J. Regnier, J. Menaucourt, A. Thomy, and X. Duval, J. Chim. Phys. **78**, 629 (1981).
[54]L. W. Bruch, J. Chem. Phys. **79**, 3148 (1983).
[55]A. Terlain and Y. Larher, Surf. Sci. **125**, 304 (1983).
[56]A. V. Kiselev and N. V. Kovaleva, Izv. Akad. Nauk. SSSR, Otd. Khim. Nauk. **1**, 989 (1959).
[57]N. M. Avgul and A. V. Kiselev, in *Chemistry and Physics of Carbon,* edited by P. Walker, Jr. (Dekker, New York, 1970), Vol. 6.